Stability Conditions for Wave Simulation in 3-D Anisotropic Media with the Pseudospectral Method

Wensheng Zhang*

LSEC, Institute of Computational Mathematics and Scientific/Engineering Computing, Academy of Mathematics and Systems Science, Chinese Academy of Sciences, P.O. Box Beijing 2719, P.R. China.

Abstract. Simulation of elastic wave propagation has important applications in many areas such as inverse problem and geophysical exploration. In this paper, stability conditions for wave simulation in 3-D anisotropic media with the pseudospectral method are investigated. They can be expressed explicitly by elasticity constants which are easy to be applied in computations. The 3-D wave simulation for two typical anisotropic media, transversely isotropic media and orthorhombic media, are carried out. The results demonstrate some satisfactory behaviors of the pseudospectral method.

AMS subject classifications: 35L05, 65C20, 65N12, 65T99, 68U20

Key words: Wave simulation, stability conditions, 3-D, anisotropic media, pseudospectral method.

1 Introduction

Forward modeling is an important way to construct synthetic data which can be used in inverse problems, it is also a valuable way for studying wave phenomenon in complex geological structures. Various techniques for wave modeling have been developed. Such methods include the ray-tracing [8, 16], finite-volume [11, 41], finite-difference [1, 12, 18, 20, 25, 36–39], finite-element [4, 6, 7, 9, 10, 22], spectral-element [5, 33] and pseudospectral methods [15, 21, 29, 30]. In this paper, the pseudospectral or Fourier method will be used.

The ray-tracing method is based on the asymptotic solution of the eikonal equation. It has the limit of high frequency assumption. The finite-volume method adapts to unstructural grids, but constructing schemes with high-order accuracy in space is not easy. The finite-difference method is a widely used method. Its main drawback is a limitation on high-frequency resolution. Usually, ten or more grid points per wavelength are required at the Nyquist spatial frequency for the second-order explicit finite-difference method [1].

---

*Corresponding author. *Email address:* `zws@lsec.cc.ac.cn` (W. S. Zhang)

For typical wave velocities and frequency bands in application such as in exploration seismology, it means that the grid space is the order of $3-4m$. The finite-element method is well known for its flexibility in describing problem with complex geometries. However, it is not commonly used in wave simulation. The main reason is that it requires to inverse mass matrix at each time step. In order to get an efficient scheme, the mass lumping technique is needed [4,9,40]. For low-order element such as linear Lagrange element, the mass lumping can be implemented by using the quadratic rules for numerical integration, but for high-order Lagrange element, it is not obvious and a new finite-element space is required [9]. Some comparisons between finite-element and finite-difference for solving the wave equation have already been given, for example, see [22] and [24]. The spectral-element method was first introduced by Patera [27] in computational fluid dynamics. It was first used for modelling wave propagation by Seriani et al. [33]. Like the finite-element method, the mass lumping is also used in the spectral-element method [5].

The pseudospectral method or Fourier method was introduced in early 1970s [13, 26]. Fornberg discussed the basic features of pseudospectral method and compared the method with the finite-difference method for the 2-D elastic wave equation [14]. He pointed out in the case of smoothly varying coefficients the required grid spacings in each space dimension satisfied ratios of $16:4:1$ for the pseudospectral method, fourth-order difference, and second-order finite-difference. The pseudospectral method differs from the finite-difference technique is that it uses the fast Fourier transform (FFT) to calculate spatial derivatives instead of finite-difference. The resulting derivative operators are highly accurate, and only two grid points are required to resolve a spatial wave length. The pseudospectral method can be viewed as the limit of finite-difference with infinite order of accuracy. Usually, high accuracy in spatial approximation is the primary pursuit in wave simulation. This is the main reason why we use the Fourier method in this paper.

Anisotropy is existed widely in the earth. For example, sedimentary rocks frequently possess an anisotropic structure [31]. In a completely anisotropic medium, 21 elastic constants are necessary to correctly define the medium [3]. Body symmetries reduce the number of independent elastic parameters. There are two typical and important anisotropic medium, transversely isotropic (TI) media and orthorhombic anisotropy (OA) media. Transversely isotropic media exhibits hexagonal symmetry that reduces to 5 the number of independent elastic constants, while OA media has 9 independent elastic constants.

In this paper, the pseudospectral or Fourier method is applied to simulating wave propagation in 3-D anisotropic media. Wave simulation with this method has been done for acoustic and elastic isotropic media [21,29,30], however, to my knowledge, the work of 3-D wave simulation in TI and OA media is few and its stability analysis is still a blank. I focus attentions on the stability analysis of 3-D numerical simulation. The stability conditions for OA and arbitrary anisotropic media are investigated. They can be expressed explicitly with elastic constants. Numerical computations for two typical 3-D anisotropic models, transversely isotropic media and orthorhombic anisotropy media, are implemented. The results show the corrects and effects of our algorithm and analysis.

2 Theory

2.1 Wavefield extrapolation scheme

The linearized set of partial differential equations which govern the displacement of anisotropic elastic solid satisfy

$$c_{ijkl}\frac{\partial^2 u_k}{\partial x_l \partial x_j} + \rho f_i = \rho \frac{\partial^2 u_i}{\partial t^2}. \tag{2.1}$$

The equations are written with respect to a fixed Cartesian reference frame $Ox_1x_2x_3$, with t denoting time. u_i denotes the components of the displacement vector. The components of the body force vector, per unit mass, are f_i and ρ is the constant density of the solid. c_{ijkl} is the fourth-order tensor of elastic constants. The symmetries reduce the number of independent elements of the elastic constants tensor c_{ijkl} from 81 to 21 which is often expressed by a 6×6 symmetric (elasticity) matrix [3, 28]. For orthorhombic anisotropy (OA) media, this elasticity constants matrix has 9 non-zero elements: c_{11}, c_{12}, c_{13}, c_{22}, c_{23}, c_{33}, c_{44}, c_{55}, c_{66}, while for transversely isotropic (TI) media, it has 5 non-zero elements: $c_{11} = c_{22}$, c_{12}, $c_{13} = c_{23}$, c_{33}, $c_{44} = c_{55}$, $c_{66} = (c_{11} - c_{12})/2$.

For convenience, we rewrite u_1, u_2 and u_3 as u, v and w respectively. Then the wave equation (2.1) in OA media becomes

$$\frac{\partial^2 u}{\partial t^2} = \frac{\partial}{\partial x_1}\left[c_{11}\frac{\partial u}{\partial x_1} + c_{12}\frac{\partial v}{\partial x_2} + c_{13}\frac{\partial w}{\partial x_3}\right] + \frac{\partial}{\partial x_3}\left[c_{55}\left(\frac{\partial w}{\partial x_1} + \frac{\partial u}{\partial x_3}\right)\right]$$
$$+ \frac{\partial}{\partial x_2}\left[c_{66}\left(\frac{\partial u}{\partial x_2} + \frac{\partial v}{\partial x_1}\right)\right] + f_1, \tag{2.2a}$$

$$\frac{\partial^2 v}{\partial t^2} = \frac{\partial}{\partial x_2}\left[c_{12}\frac{\partial u}{\partial x_1} + c_{22}\frac{\partial v}{\partial x_2} + c_{23}\frac{\partial w}{\partial x_3}\right] + \frac{\partial}{\partial x_3}\left[c_{44}\left(\frac{\partial v}{\partial x_3} + \frac{\partial w}{\partial x_2}\right)\right]$$
$$+ \frac{\partial}{\partial x_1}\left[c_{66}\left(\frac{\partial u}{\partial x_2} + \frac{\partial v}{\partial x_1}\right)\right] + f_2, \tag{2.2b}$$

$$\frac{\partial^2 w}{\partial t^2} = \frac{\partial}{\partial x_3}\left[c_{13}\frac{\partial u}{\partial x_1} + c_{23}\frac{\partial v}{\partial x_2} + c_{33}\frac{\partial w}{\partial x_3}\right] + \frac{\partial}{\partial x_2}\left[c_{44}\left(\frac{\partial v}{\partial x_3} + \frac{\partial w}{\partial x_2}\right)\right]$$
$$+ \frac{\partial}{\partial x_1}\left[c_{55}\left(\frac{\partial w}{\partial x_1} + \frac{\partial u}{\partial x_3}\right)\right] + f_3. \tag{2.2c}$$

Here, c_{ij} are density-normalized stiffness and thus are of dimension velocity^2. In general, the stiffness are constrained by the conditions of stability of the medium, i.e., the condition that the 6×6 matrix with elements c_{ij} is positive definite. In the following, we assume c_{ij} are constants, i.e., the medium is homogeneous. However, the derived result can be used for inhomogeneous media such as the media with piecewise elastic constants. If we approximate the second-order derivatives of time with the second-order finite-difference

scheme, and calculate the space derivatives with the fast Fourier transform, we will get the following wavefield extrapolation scheme

$$U^{n+1} = -U^{n-1} + 2U^n - \Delta t^2 (c_{11}k_1^2 + c_{66}k_2^2 + c_{55}k_3^2)U^n - \Delta t^2 (c_{12}+c_{66})k_1k_2 V^n$$
$$- \Delta t^2 (c_{13}+c_{55})k_1k_3 W^n, \tag{2.3a}$$

$$V^{n+1} = -V^{n-1} + 2V^n - \Delta t^2 (c_{12}+c_{66})k_1k_2 U^n - \Delta t^2 (c_{66}k_1^2 + c_{22}k_2^2 + c_{44}k_3^2)V^n$$
$$- \Delta t^2 (c_{23}+c_{44})k_2k_3 W^n, \tag{2.3b}$$

$$W^{n+1} = -W^{n-1} + 2W^n - \Delta t^2 (c_{13}+c_{55})k_1k_3 U^n - \Delta t^2 (c_{23}+c_{44})k_2k_3 V^n$$
$$- \Delta t^2 (c_{55}k_1^2 + c_{44}k_2^2 + c_{33}k_3^2)W^n, \tag{2.3c}$$

where U,V,W are the corresponding results of spatial Fourier transform of u,v,w respectively. k_1, k_2 and k_3 are the spatial wavenumber of x, y and z respectively. Eq. (2.3) is the scheme for wavefield extrapolation in time.

2.2 Stability condition for OA media

Rewrite (2.3) as a matrix form

$$
\begin{bmatrix} U^{n+1} \\ U^n \\ V^{n+1} \\ V^n \\ W^{n+1} \\ W^n \end{bmatrix} =
\begin{bmatrix}
2+\theta_1 & -1 & \theta_4 & 0 & \theta_5 & 0 \\
1 & 0 & 0 & 0 & 0 & 0 \\
\theta_4 & 0 & 2+\theta_2 & -1 & \theta_6 & 0 \\
0 & 0 & 1 & 0 & 0 & 0 \\
\theta_5 & 0 & \theta_6 & 0 & 2+\theta_3 & -1 \\
0 & 0 & 0 & 0 & 1 & 0
\end{bmatrix}
\begin{bmatrix} U^n \\ U^{n-1} \\ V^n \\ V^{n-1} \\ W^n \\ W^{n-1} \end{bmatrix}. \tag{2.4}
$$

To analyze the stability condition, we consider the characteristic equation of the transfer matrix in (2.4). The characteristic equation is

$$\lambda^6 + A_5\lambda^5 + A_4\lambda^4 + A_3\lambda^3 + A_2\lambda^2 + A_1\lambda + 1 = 0, \tag{2.5}$$

where

$$A_5 = A_1 = -(\mu_1+\mu_2+\mu_3),$$
$$A_4 = A_2 = (3+\mu_1\mu_2+\mu_1\mu_3+\mu_2\mu_3) - (\theta_4^2+\theta_5^2+\theta_6^2),$$
$$A_3 = -2(\mu_1+\mu_2+\mu_3) + \mu_3\theta_4^2 + \mu_2\theta_5^2 + \mu_1\theta_6^2 - 2\theta_4\theta_5\theta_6 - \mu_1\mu_2\mu_3,$$

with

$$\mu_i = 2 + \theta_i, \qquad i = 1,2,3, \tag{2.6}$$

and

$$\theta_1 = -\Delta t^2 (c_{11}k_1^2 + c_{66}k_2^2 + c_{55}k_3^2), \qquad \theta_4 = -\Delta t^2 (c_{12}+c_{66})k_1k_2, \tag{2.7a}$$
$$\theta_2 = -\Delta t^2 (c_{66}k_1^2 + c_{22}k_2^2 + c_{44}k_3^2), \qquad \theta_5 = -\Delta t^2 (c_{13}+c_{55})k_1k_3, \tag{2.7b}$$
$$\theta_3 = -\Delta t^2 (c_{55}k_1^2 + c_{44}k_2^2 + c_{33}k_3^2), \qquad \theta_6 = -\Delta t^2 (c_{23}+c_{44})k_2k_3. \tag{2.7c}$$

The necessary condition of stability for wavefield extrapolation in time is $|\lambda_i| \leqslant 1$, $i = 1$, $2, \cdots, 6$. From the relationship between roots λ_i and coefficients A_i, we have the restriction of $|\lambda_i| = 1$ ($i = 1, 2, \cdots, 6$). Otherwise, at least one root will be out of the unit circle and lead to unstability [23, 34]. Obviously, the six characteristic roots will be in pair and so (2.5) can be factorized as

$$(\lambda^2 + r_1\lambda + 1)(\lambda^2 + r_2\lambda + 1)(\lambda^2 + r_3\lambda + 1) = 0, \tag{2.8}$$

where r_i ($i = 1, 2, 3$) are real coefficients and can be determined but not necessary here. Expanding (2.8) and comparing the result with (2.5) yield the following expressions

$$r_1 + r_2 + r_3 = A_5, \tag{2.9a}$$
$$3 + r_1 r_2 + r_2 r_3 + r_1 r_3 = A_4, \tag{2.9b}$$
$$r_1 r_2 r_3 + 2(r_1 + r_2 + r_3) = A_3. \tag{2.9c}$$

Therefore, based on (2.9a)-(2.9c) and the restriction of $|\lambda_i| = 1$, we obtain the following inequalities

$$|A_5| \leqslant 6, \qquad |A_4 - 3| \leqslant 12, \qquad |A_3 - 2A_5| \leqslant 8. \tag{2.10}$$

From the first inequality in (2.10), we have

$$-12 \leqslant \theta_1 + \theta_2 + \theta_3 \leqslant 0, \tag{2.11}$$

or

$$\Delta t^2 \left[k_1^2 (c_{11} + c_{55} + c_{66}) + k_2^2 (c_{22} + c_{44} + c_{66}) + k_3^2 (c_{33} + c_{44} + c_{55}) \right] \leqslant 12. \tag{2.12}$$

According to the sampling theorem [19], the maximum of wave number k_1, k_2 and k_3 are $\pi/\Delta x$, $\pi/\Delta y$ and $\pi/\Delta z$ respectively. Here, Δx, Δy and Δz are the spatial steps with respect to x, y and z respectively. Thus (2.12) yields the first restriction of Δt as

$$\Delta t_1 \leqslant \frac{\sqrt{12}}{\pi \sqrt{\frac{c_{11} + c_{55} + c_{66}}{\Delta x^2} + \frac{c_{22} + c_{44} + c_{66}}{\Delta y^2} + \frac{c_{33} + c_{44} + c_{55}}{\Delta z^2}}}. \tag{2.13}$$

From the second inequality in (2.10), we have

$$\left| \mu_1 \mu_2 + \mu_1 \mu_3 + \mu_2 \mu_3 - (\theta_4^2 + \theta_5^2 + \theta_6^2) \right| \leqslant 12, \tag{2.14}$$

i.e,

$$-24 \leqslant 4(\theta_1 + \theta_2 + \theta_3) + \theta_1 \theta_2 + \theta_1 \theta_3 + \theta_2 \theta_3 - (\theta_4^2 + \theta_5^2 + \theta_6^2) \leqslant 0. \tag{2.15}$$

Using the relationship (2.11), we obtain

$$\frac{1}{2}(\theta_1^2 + \theta_2^2 + \theta_3^2) + (\theta_4^2 + \theta_5^2 + \theta_6^2) \leqslant 96, \tag{2.16}$$

which yields the second restriction for the time step

$$\Delta t_2 \leqslant \frac{2\sqrt[4]{6}}{\pi}\left\{\frac{1}{2}\left(\frac{c_{11}}{\Delta x^2}+\frac{c_{66}}{\Delta y^2}+\frac{c_{55}}{\Delta z^2}\right)^2+\frac{1}{2}\left(\frac{c_{66}}{\Delta x^2}+\frac{c_{22}}{\Delta y^2}+\frac{c_{44}}{\Delta z^2}\right)^2+\frac{1}{2}\left(\frac{c_{55}}{\Delta x^2}+\frac{c_{44}}{\Delta y^2}+\frac{c_{33}}{\Delta z^2}\right)^2\right.$$
$$\left.+\frac{(c_{12}+c_{66})^2}{\Delta x^2\Delta y^2}+\frac{(c_{13}+c_{55})^2}{\Delta x^2\Delta z^2}+\frac{(c_{23}+c_{44})^2}{\Delta y^2\Delta z^2}\right\}^{-\frac{1}{4}}. \tag{2.17}$$

From the third inequity in (2.10), we conclude

$$0\leqslant 2(\theta_4^2+\theta_5^2+\theta_6^2)+\theta_3\theta_4^2+\theta_2\theta_5^2+\theta_1\theta_6^2-2\theta_4\theta_5\theta_6$$
$$-2(\theta_1\theta_2+\theta_1\theta_3+\theta_2\theta_3)-4(\theta_1+\theta_2+\theta_3)-\theta_1\theta_2\theta_3\leqslant 16. \tag{2.18}$$

Using the following relationships from (2.11) and (2.16):

$$-48\leqslant 4(\theta_1+\theta_2+\theta_3)\leqslant 0, \tag{2.19a}$$
$$-192\leqslant -(\theta_1^2+\theta_2^2+\theta_3^2)-2(\theta_4^2+\theta_5^2+\theta_6^2)\leqslant 0, \tag{2.19b}$$
$$0\leqslant \theta_1^2+\theta_2^2+\theta_3^2+2(\theta_1\theta_2+\theta_1\theta_3+\theta_2\theta_3)\leqslant 144, \tag{2.19c}$$

we have

$$-240\leqslant \theta_3\theta_4^2+\theta_2\theta_5^2+\theta_1\theta_6^2-2\theta_4\theta_5\theta_6-\theta_1\theta_2\theta_3\leqslant 160. \tag{2.20}$$

Considering the stability of media, we obtain the third restriction for the time interval

$$\Delta t_3 \leqslant \frac{\sqrt[6]{160}}{\pi}\left\{\left(\frac{c_{55}}{\Delta x^2}+\frac{c_{44}}{\Delta y^2}+\frac{c_{33}}{\Delta z^2}\right)\frac{(c_{12}+c_{66})^2}{\Delta x^2\Delta y^2}+\left(\frac{c_{66}}{\Delta x^2}+\frac{c_{22}}{\Delta y^2}+\frac{c_{44}}{\Delta z^2}\right)\frac{(c_{13}+c_{55})^2}{\Delta x^2\Delta z^2}\right.$$
$$+\left(\frac{c_{11}}{\Delta x^2}+\frac{c_{66}}{\Delta y^2}+\frac{c_{55}}{\Delta z^2}\right)\frac{(c_{23}+c_{44})^2}{\Delta y^2\Delta z^2}-\frac{2(c_{12}+c_{66})(c_{13}+c_{55})(c_{23}+c_{44})}{\Delta x^2\Delta y^2\Delta z^2}$$
$$\left.-\left(\frac{c_{11}}{\Delta x^2}+\frac{c_{66}}{\Delta y^2}+\frac{c_{55}}{\Delta z^2}\right)\left(\frac{c_{66}}{\Delta x^2}+\frac{c_{22}}{\Delta y^2}+\frac{c_{44}}{\Delta z^2}\right)\left(\frac{c_{55}}{\Delta x^2}+\frac{c_{44}}{\Delta y^2}+\frac{c_{33}}{\Delta z^2}\right)\right\}^{-\frac{1}{6}}. \tag{2.21}$$

If the grids are uniform i.e., $\Delta x=\Delta y=\Delta z:=h$, (2.13), (2.17) and (2.21) are simplified as

$$\Delta t_1 \leqslant \frac{\sqrt{2}h}{\pi\sqrt{c_{11}+c_{22}+c_{33}+2(c_{44}+c_{55}+c_6)}}, \tag{2.22a}$$

$$\Delta t_2 \leqslant \frac{2\sqrt[4]{6}h}{\pi}\left\{\frac{1}{2}(c_{11}+c_{66}+c_{55})^2+\frac{1}{2}(c_{66}+c_{22}+c_{44})^2+\frac{1}{2}(c_{55}+c_{44}+c_{33})^2\right.$$
$$\left.+(c_{13}+c_{66})^2+(c_{13}+c_{55})^2+(c_{23}+c_{44})^2\right\}^{-\frac{1}{4}}, \tag{2.22b}$$

$$\Delta t_3 \leqslant \frac{\sqrt[6]{160}h}{\pi}\left\{(c_{55}+c_{44}+c_{33})(c_{12}+c_{66})^2+(c_{66}+c_{22}+c_{44})(c_{13}+c_{55})^2\right.$$
$$+(c_{11}+c_{66}+c_{55})(c_{23}+c_{44})^2-2(c_{12}+c_{66})(c_{13}+c_{55})(c_{23}+c_{44})$$
$$\left.-(c_{11}+c_{55}+c_{66})(c_{22}+c_{44}+c_{66})(c_{33}+c_{44}+c_{55})\right\}^{-\frac{1}{6}}, \tag{2.22c}$$

respectively. Combing (2.13), (2.17) and (2.21) or (2.22a), (2.22b) and (2.22c), we obtain following stability condition for OA media

$$\Delta t < \min\{\Delta t_1, \Delta t_2, \Delta t_3\}. \tag{2.23}$$

The TI media can be treated as a special case of OA media, so its stability condition can be obtained from (2.23) with relationships $c_{11} = c_{22}$, $c_{13} = c_{23}$, $c_{44} = c_{55}$ and $c_{66} = (c_{11} - c_{12})/2$. Similarly, the stability condition for elastic isotropic media can also be obtained from (2.23) with relationships $c_{11} = c_{22} = c_{33} = v_p^2$, $c_{44} = c_{55} = c_{66} = v_s^2$ and $c_{12} = c_{13} = c_{11} - 2c_{44}$, where v_p and v_s are the compress wave velocity and the shear wave velocity respectively.

2.3 Stability condition for arbitrary anisotropic media

In this section, I will generalize the stability condition to arbitrary anisotropic media. For arbitrary anisotropic media, there are 21 elasticity constants. Without loss of generality in the following, we rewrite x_1, x_2 and x_3 as x, y and z respectively. In the domain of wave number, the wave equation (2.1) without source can be written as

$$\frac{\partial^2 P}{\partial t^2}(K,t) = -MP(K,t), \tag{2.24}$$

where $P = (U, V, W)$ is the wavefield in the wave number domain corresponding to its spatial domain, $K = (k_x, k_y, k_z)$ and M is given by

$$M = \begin{bmatrix} \beta_1 & \beta_4 & \beta_5 \\ \beta_4 & \beta_2 & \beta_6 \\ \beta_5 & \beta_6 & \beta_3 \end{bmatrix} \tag{2.25}$$

with

$$\beta_1 = c_{11}k_x^2 + c_{66}k_y^2 + c_{55}k_z^2 + 2c_{16}k_xk_y + 2c_{56}k_yk_z + 2c_{15}k_xk_z, \tag{2.26a}$$

$$\beta_2 = c_{66}k_x^2 + c_{22}k_y^2 + c_{44}k_z^2 + 2c_{26}k_xk_y + 2c_{24}k_yk_z + 2c_{46}k_xk_z, \tag{2.26b}$$

$$\beta_3 = c_{55}k_x^2 + c_{44}k_y^2 + c_{33}k_z^2 + 2c_{45}k_xk_y + 2c_{34}k_yk_z + 2c_{35}k_xk_z, \tag{2.26c}$$

$$\beta_4 = c_{16}k_x^2 + c_{26}k_y^2 + c_{45}k_z^2 + (c_{12}+c_{66})k_xk_y + (c_{25}+c_{46})k_yk_z + (c_{14}+c_{56})k_xk_z, \tag{2.26d}$$

$$\beta_5 = c_{15}k_x^2 + c_{46}k_y^2 + c_{35}k_z^2 + (c_{14}+c_{56})k_xk_y + (c_{36}+c_{45})k_yk_z + (c_{13}+c_{55})k_xk_z, \tag{2.26e}$$

$$\beta_6 = c_{56}k_x^2 + c_{24}k_y^2 + c_{34}k_z^2 + (c_{25}+c_{46})k_xk_y + (c_{23}+c_{44})k_yk_z + (c_{36}+c_{55})k_xk_z, \tag{2.26f}$$

where k_x, k_y and k_z are the spatial wave number with respect to x, y, z respectively.

The extrapolation scheme for (2.24) with the pseudospectral method can be written as

$$\begin{bmatrix} U^{n+1} \\ U^n \\ V^{n+1} \\ V^n \\ W^{n+1} \\ W^n \end{bmatrix} = \begin{bmatrix} 2+\beta_1 & -1 & \beta_4 & 0 & \beta_5 & 0 \\ 1 & 0 & 0 & 0 & 0 & 0 \\ \beta_4 & 0 & 2+\beta_2 & -1 & \beta_6 & 0 \\ 0 & 0 & 1 & 0 & 0 & 0 \\ \beta_5 & 0 & \beta_6 & 0 & 2+\beta_3 & -1 \\ 0 & 0 & 0 & 0 & 1 & 0 \end{bmatrix} \begin{bmatrix} U^n \\ U^{n-1} \\ V^n \\ V^{n-1} \\ W^n \\ W^{n-1} \end{bmatrix}. \tag{2.27}$$

The characteristic equation of the transfer matrix in (2.27) is

$$\lambda^6 + B_5\lambda^5 + B_4\lambda^4 + B_3\lambda^3 + B_2\lambda^2 + B_1\lambda + 1 = 0, \tag{2.28}$$

where

$$B_5 = B_1 = -(\gamma_1 + \gamma_2 + \gamma_3), \tag{2.29a}$$

$$B_4 = B_2 = (3 + \gamma_1\gamma_2 + \gamma_1\gamma_3 + \gamma_2\gamma_3) - (\beta_4^2 + \beta_5^2 + \beta_6^2), \tag{2.29b}$$

$$B_3 = -2(\gamma_1 + \gamma_2 + \gamma_3) + \gamma_3\beta_4^2 + \gamma_2\beta_5^2 + \gamma_1\beta_6^2 - 2\beta_4\beta_5\beta_6 - \gamma_1\gamma_2\gamma_3, \tag{2.29c}$$

with

$$\gamma_i = 2 + \beta_i, \qquad i = 1, 2, 3. \tag{2.30}$$

Using the similar approach in Section 2.2, the stability condition for arbitrary anisotropic media requires

$$|B_5| \leqslant 6, \qquad |B_4 - 3| \leqslant 12, \qquad |B_3 - 2B_5| \leqslant 8. \tag{2.31}$$

Through a series of deduction similar to that in the Section 2.2, we conclude the stability condition for arbitrary media media is

$$\Delta t < \min\{\Delta t_1, \Delta t_2, \Delta t_3\}, \tag{2.32}$$

where

$$\Delta t_1 < \frac{\sqrt{12}}{\pi} \left\{ \frac{c_{11} + c_{55} + c_{66}}{\Delta x^2} + \frac{c_{22} + c_{44} + c_{66}}{\Delta y^2} + \frac{c_{33} + c_{44} + c_{55}}{\Delta z^2} + \frac{2(c_{16} + c_{26} + c_{45})}{\Delta x \Delta y} \right.$$
$$\left. + \frac{2(c_{24} + c_{34} + c_{56})}{\Delta y \Delta z} + \frac{2(c_{15} + c_{35} + c_{46})}{\Delta x \Delta z} \right\}^{-1/2}, \tag{2.33a}$$

$$\Delta t_2 \leqslant \frac{2\sqrt[4]{6}}{\pi} \left\{ \frac{1}{2} \left(\frac{c_{11}}{\Delta x^2} + \frac{c_{66}}{\Delta y^2} + \frac{c_{55}}{\Delta z^2} + \frac{2c_{16}}{\Delta x \Delta y} + \frac{2c_{56}}{\Delta y \Delta z} + \frac{2c_{15}}{\Delta x \Delta z} \right)^2 \right.$$

$$+ \frac{1}{2} \left(\frac{c_{66}}{\Delta x^2} + \frac{c_{22}}{\Delta y^2} + \frac{c_{44}}{\Delta z^2} + \frac{2c_{26}}{\Delta x \Delta y} + \frac{2c_{24}}{\Delta y \Delta z} + \frac{2c_{46}}{\Delta x \Delta z} \right)^2$$

$$+ \frac{1}{2} \left(\frac{c_{55}}{\Delta x^2} + \frac{c_{44}}{\Delta y^2} + \frac{c_{33}}{\Delta z^2} + \frac{2c_{45}}{\Delta x \Delta y} + \frac{2c_{34}}{\Delta y \Delta z} + \frac{2c_{35}}{\Delta x \Delta z} \right)^2$$

$$+ \left[\frac{c_{16}}{\Delta x^2} + \frac{c_{26}}{\Delta y^2} + \frac{c_{45}}{\Delta z^2} + \frac{(c_{12} + c_{66})}{\Delta x \Delta y} + \frac{(c_{25} + c_{46})}{\Delta y \Delta z} + \frac{(c_{14} + c_{56})}{\Delta x \Delta z} \right]^2$$

$$+ \left[\frac{c_{15}}{\Delta x^2} + \frac{c_{46}}{\Delta y^2} + \frac{c_{35}}{\Delta z^2} + \frac{(c_{14} + c_{56})}{\Delta x \Delta y} + \frac{(c_{36} + c_{45})}{\Delta y \Delta z} + \frac{(c_{13} + c_{55})}{\Delta x \Delta z} \right]^2$$

$$+ \left. \left[\frac{c_{56}}{\Delta x^2} + \frac{c_{26}}{\Delta y^2} + \frac{c_{34}}{\Delta z^2} + \frac{(c_{25} + c_{46})}{\Delta x \Delta y} + \frac{(c_{23} + c_{44})}{\Delta y \Delta z} + \frac{(c_{36} + c_{55})}{\Delta x \Delta z} \right]^2 \right\}^{-\frac{1}{4}}, \tag{2.33b}$$

$$
\begin{aligned}
\Delta t_3 \leqslant \frac{\sqrt[6]{160}}{\pi} \Bigg\{ &\left(\frac{c_{55}}{\Delta x^2} + \frac{c_{44}}{\Delta y^2} + \frac{c_{33}}{\Delta z^2} + \frac{2c_{45}}{\Delta x \Delta y} + \frac{2c_{34}}{\Delta y \Delta z} + \frac{2c_{35}}{\Delta x \Delta z} \right) \\
&\times \left[\frac{c_{16}}{\Delta x^2} + \frac{c_{26}}{\Delta y^2} + \frac{c_{45}}{\Delta z^2} + \frac{(c_{12}+c_{66})}{\Delta x \Delta y} + \frac{(c_{25}+c_{46})}{\Delta y \Delta z} + \frac{(c_{14}+c_{56})}{\Delta x \Delta z} \right]^2 \\
&+ \left(\frac{c_{66}}{\Delta x^2} + \frac{c_{22}}{\Delta y^2} + \frac{c_{44}}{\Delta z^2} + \frac{2c_{26}}{\Delta x \Delta y} + \frac{2c_{24}}{\Delta y \Delta z} + \frac{2c_{46}}{\Delta x \Delta z} \right) \\
&\times \left[\frac{c_{15}}{\Delta x^2} + \frac{c_{46}}{\Delta y^2} + \frac{c_{35}}{\Delta z^2} + \frac{(c_{14}+c_{56})}{\Delta x \Delta y} + \frac{(c_{36}+c_{45})}{\Delta y \Delta z} + \frac{(c_{13}+c_{55})}{\Delta x \Delta z} \right]^2 \\
&+ \left(\frac{c_{11}}{\Delta x^2} + \frac{c_{66}}{\Delta y^2} + \frac{c_{55}}{\Delta z^2} + \frac{2c_{16}}{\Delta x \Delta y} + \frac{2c_{56}}{\Delta y \Delta z} + \frac{2c_{15}}{\Delta x \Delta z} \right) \\
&\times \left[\frac{c_{56}}{\Delta x^2} + \frac{c_{26}}{\Delta y^2} + \frac{c_{34}}{\Delta z^2} + \frac{(c_{25}+c_{46})}{\Delta x \Delta y} + \frac{(c_{23}+c_{44})}{\Delta y \Delta z} + \frac{(c_{36}+c_{55})}{\Delta x \Delta z} \right]^2 \\
&- 2 \left[\frac{c_{16}}{\Delta x^2} + \frac{c_{26}}{\Delta y^2} + \frac{c_{45}}{\Delta z^2} + \frac{(c_{12}+c_{66})}{\Delta x \Delta y} + \frac{(c_{25}+c_{46})}{\Delta y \Delta z} + \frac{(c_{14}+c_{55})}{\Delta x \Delta z} \right] \\
&\times \left[\frac{c_{15}}{\Delta x^2} + \frac{c_{46}}{\Delta y^2} + \frac{c_{35}}{\Delta z^2} + \frac{(c_{14}+c_{56})}{\Delta x \Delta y} + \frac{(c_{36}+c_{45})}{\Delta y \Delta z} + \frac{(c_{13}+c_{55})}{\Delta x \Delta z} \right] \\
&\times \left[\frac{c_{56}}{\Delta x^2} + \frac{c_{24}}{\Delta y^2} + \frac{c_{34}}{\Delta z^2} + \frac{(c_{25}+c_{46})}{\Delta x \Delta y} + \frac{(c_{23}+c_{44})}{\Delta y \Delta z} + \frac{(c_{36}+c_{55})}{\Delta x \Delta z} \right] \\
&- \left(\frac{c_{11}}{\Delta x^2} + \frac{c_{66}}{\Delta y^2} + \frac{c_{55}}{\Delta z^2} + \frac{2c_{16}}{\Delta x \Delta y} + \frac{2c_{56}}{\Delta y \Delta z} + \frac{2c_{15}}{\Delta x \Delta z} \right) \\
&\times \left(\frac{c_{66}}{\Delta x^2} + \frac{c_{22}}{\Delta y^2} + \frac{c_{44}}{\Delta z^2} + \frac{2c_{26}}{\Delta x \Delta y} + \frac{2c_{24}}{\Delta y \Delta z} + \frac{2c_{46}}{\Delta x \Delta z} \right) \\
&\times \left(\frac{c_{55}}{\Delta x^2} + \frac{c_{44}}{\Delta y^2} + \frac{c_{33}}{\Delta z^2} + \frac{2c_{45}}{\Delta x \Delta y} + \frac{2c_{34}}{\Delta y \Delta z} + \frac{2c_{35}}{\Delta x \Delta z} \right) \Bigg\}^{-\frac{1}{6}},
\end{aligned}
\tag{2.33c}
$$

respectively.

3 Numerical computations

In this part, we use the pseudospectral method to simulate wave propagation in two important anisotropic media, TI media and OA media. Though the selected media are homogeneous in our computations, the pseudospectral method can be used for inhomogeneous media or other complex models. An example for a TI medium with complex structures can be found in [42]. The source function used in numerical computations is the wavelet source depicted by

$$
f(t) = \cos(2\pi f_0 t) e^{-\alpha(t-t_0)^2},
\tag{3.1}
$$

where f_0 is the main frequency, t_0 and α are the given parameters. In our computations, we choose $f_0 = 20$Hz, $t_0 = 0.06s$ and $\alpha = 4000$. Its history is shown in Fig. 1. The point
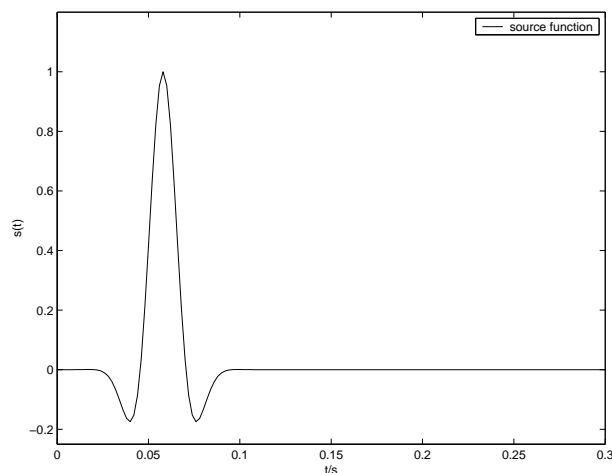
Figure 1: Source function used in numerical computations. It has 20Hz main frequency.

source is always located at the center of physical model.

First we consider 3-D wave propagation in a transversely isotropic model with a vertical symmetry axis in the z direction. The transverse plane is the xy plane. The physical model has grids of $128 \times 128 \times 128$ with uniform spatial sampling interval $h := \Delta x = \Delta y = \Delta z = 25m$. The density-normalized elastic constants are listed in Table 1. The stability condition (2.22a) gives (unit: ms)

$$\Delta t < 0.1167h \tag{3.2}$$

which requires $\Delta t < 2.9170ms$ for this medium. In the computations we choose $\Delta t = 0.002s$.

Table 1: Density-normalized elastic constants (unit: $10^6 m^2/s^2$) for a transversely medium.

c_{11}	c_{12}	c_{13}	c_{33}	c_{44}
16.7	1.31	6.6	14.0	6.63

Fig. 2 is the snapshot of 3-D wave propagation of w component at propagation time of $0.38s$. The result is completed on a PC with one processor and 3G main frequency. The cup time for this model is 33 minutes for extrapolating 250 time steps. The algorithm of Fast Fourier transform is used in computation. The wave is generated by a z (or x_3) directional point source with time function given by (3.1). Similar 3-D data volume for u and v components can also be obtained but we omit them here for reason of space. Fig. 3 shows a 2-D $x-z$ u component in the xz plane sliced at $y = 50$. The wavefront of u component can also be calculated analytically [28]. Fig. 4 is the corresponding result obtained by the analytical method. The source is also a z directional force. The outer ellipse in Fig. 4 is the qP wave. The qSV motion has four cuspidal triangles. Comparisons between Fig. 3 and Fig. 4 show the good accuracy of the pseudospectral or Fourier method.

If we slice the 3-D data volume along different directions, we can get different 2-D sections. Fig. 5, Fig. 6 and Fig. 7 are wave snapshots of three components in the xy, yz
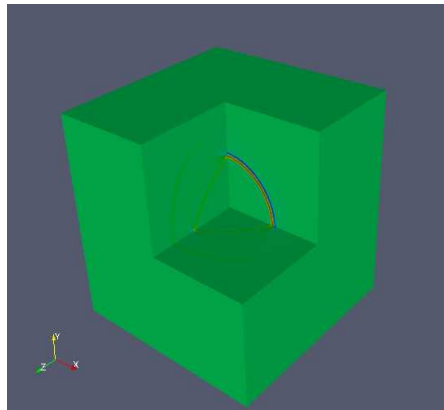
Figure 2: Snapshot of 3-D wave propagation in a transversely isotropic medium at propagation time of $0.38s$. It is a 3-D data volume of w component.
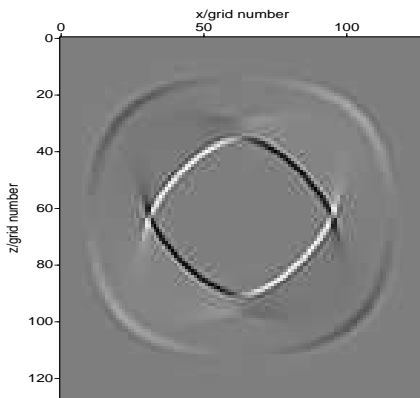

Figure 3: A snapshot of displacement u component at propagation time of $0.38s$ in transversely isotropic media. It is a 2-D $x-z$ section of the 3-D date volume.
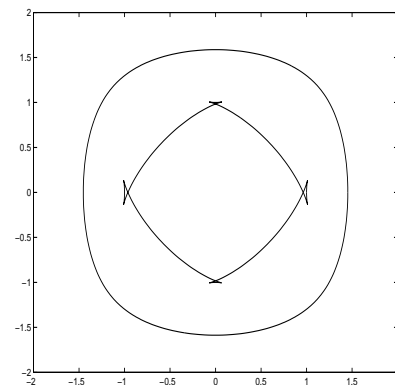

Figure 4: Wavefront of wave propagation in a transversely isotropic medium in xz plane. It is obtained by analytical method.

and xz planes respectively. In Fig. 5, wave surface sections are circles because of isotropy in the xy plane. The inner wavefront corresponds to the qSV mode. The outer wavefront is qP wave and the middle is the SH motion. In Fig. 6 and Fig. 7, all components only have qP and qSV wavefronts since SH motion is normal to the yz and xz planes when the source is the z directional point force. The qSV wavefronts have cusps and triplications [12] which can be clearly observed in Fig. 6 and Fig. 7.

It is noticed that the components are relevant to the source directions. In stead of z direction only, the source is now set in the x, y and z directions simultaneously. Fig. 8, Fig. 9 and Fig. 10 show wavefield snapshots of three components in the xy, yz and xz planes respectively. Three wave modes qP,qSV and SH are still circles in Fig. 8. The SH wave can be observed now in Fig. 9(a), Fig. 9(b), Fig. 10(a) and Fig. 10(b), which can be compared with Fig. 6(a), Fig. 6(b), Fig. 7(a) and Fig. 7(b). The wavefront of SH wave is
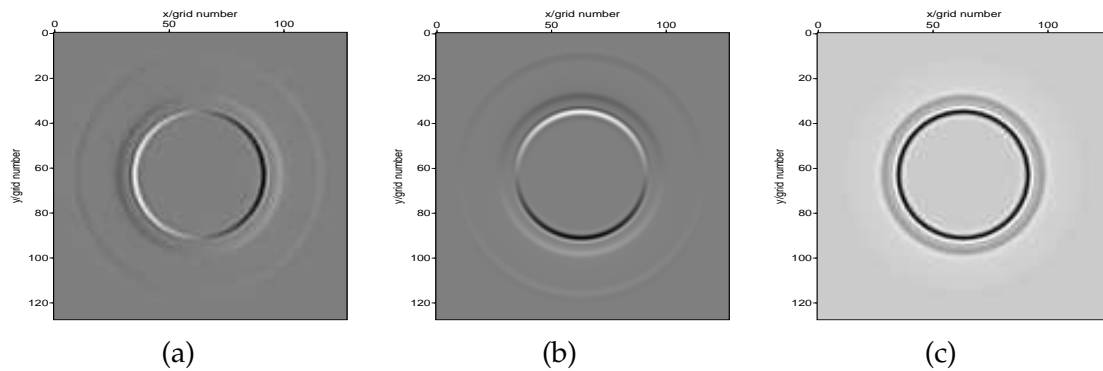
Figure 5: Wavefront of wave propagation in transversely isotropic medium in the xy plane with the z directional point source. (a) x component, (b) y component, (c) z component.
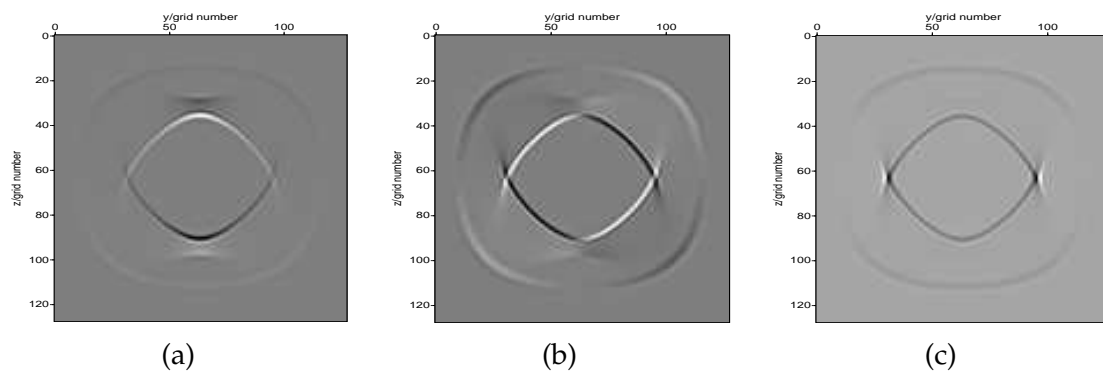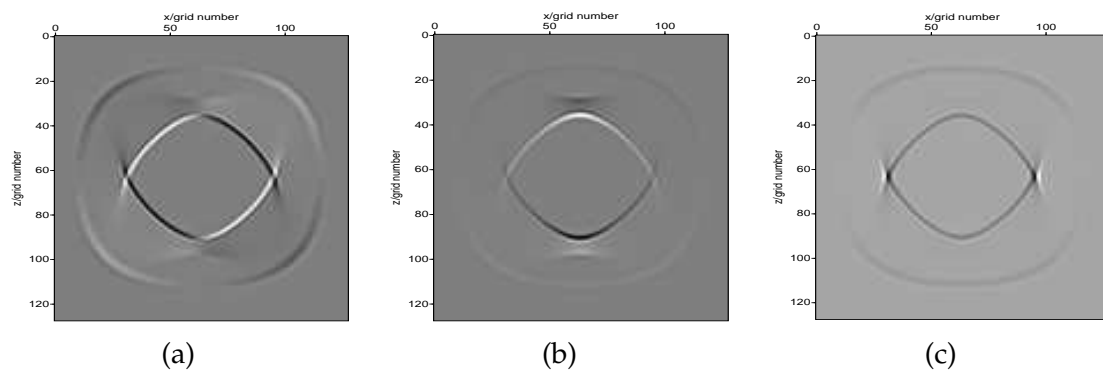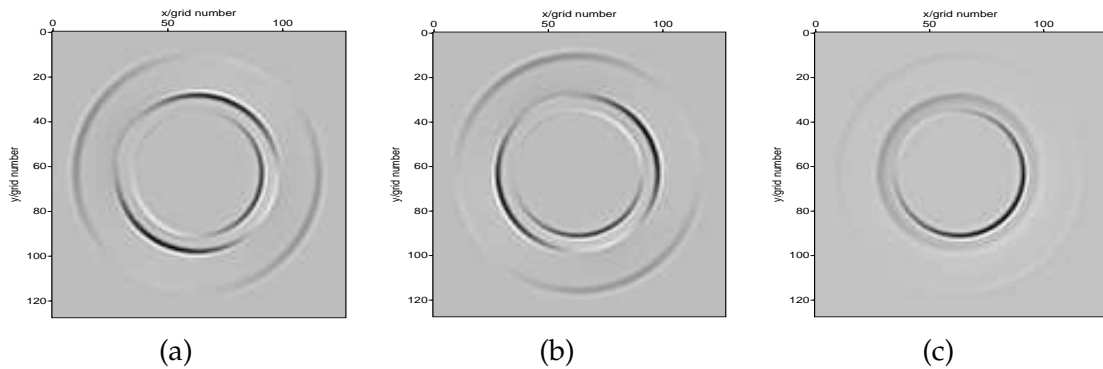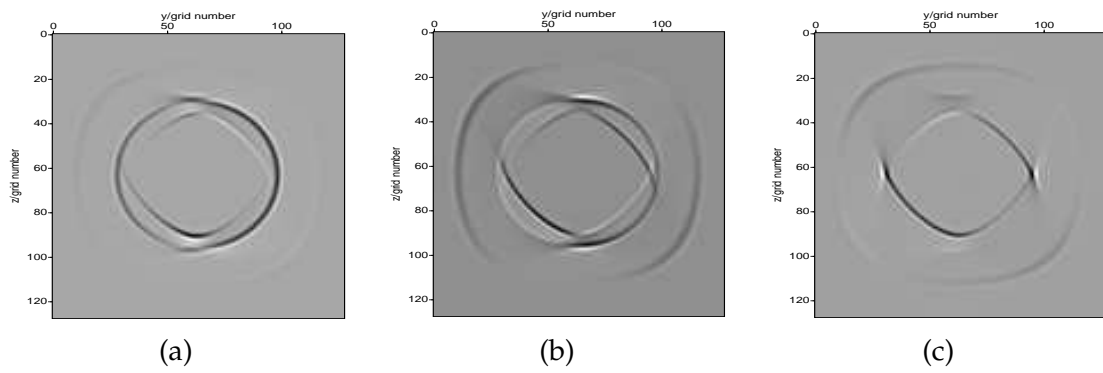

Figure 6: Wavefront of wave propagation in a transversely isotropic medium in the yz plane with the z directional point source. (a) x component, (b) y component, (c) z component.

Figure 7: Wavefront of wave propagation in a transversely isotropic medium in the xz plane with the z directional point source. (a) x component, (b) y component, (c) z component.

ellipse and the qP and qSV show the directional dependence on propagation velocity. The shear-wave splitting in Fig. 9(a), Fig. 9(b), Fig. 10(a) and Fig. 10(b) can be observed clearly.
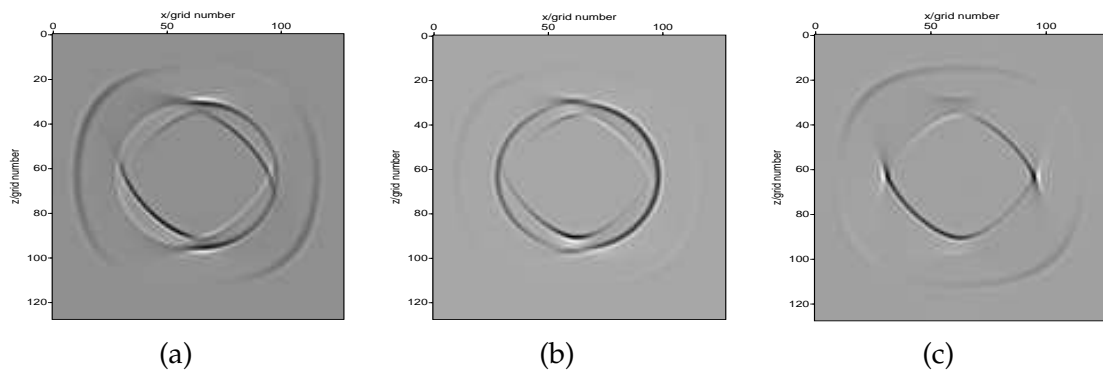
Figure 8: Wavefront of wave propagation in a transversely isotropic medium in the xy plane with three directional point source. (a) x component, (b) y component, (c) z component.

Figure 9: Wavefront of wave propagation in a transversely isotropic medium in the yz plane with three directional point source. (a) x component, (b) y component, (c) z component.

Figure 10: Wavefront of wave propagation in a transversely isotropic medium in the xz plane with three directional point source. (a) x component, (b) y component, (c)z component.

Now we simulate 3-D wave propagation in an OA medium. The density-normalized elastic constants are listed in Table 2. The physical model has the 128 grids in each dimension. In computations we choose uniform spatial steps $h := \Delta x = \Delta y = \Delta z = 20m$. The

Table 2: Density-normalized elastic constants (unit: $10^6 m^2/s^2$) for an orthorhombic anisotropic medium.

c_{11}	c_{12}	c_{13}	c_{22}	c_{23}	c_{33}	c_{44}	c_{55}	c_{66}
9.0	3.5	2.5	8.0	1.5	6.0	5.0	4.0	3.0

stability condition (2.22a) requires (unit: ms)

$$\Delta t < 0.1608h \qquad (3.3)$$

i.e., $\Delta t < 3.2168ms$, we choose $\Delta t = 2ms$. Fig. 11 is the snapshot of 3-D wave propagation which corresponds to w component at propagation time of 0.38s. The wavefront of 3-D propagation is clear in Fig. 11. The sections in three planes can be obtained from the 3-D data volume. Fig. 12, Fig. 13 and Fig. 14 show the wave snapshots of three components in the xy, yz and xz planes respectively. In Fig. 12, the wavefronts of qP, qSV and SH modes are not circles comparing with Fig. 5 and Fig. 8. The shear-splitting with triplication in the OA medium is more complicated than that in the TI medium by comparing Fig. 13(a), Fig. 13(b), Fig. 14(a), Fig. 14(b) with Fig. 9(a), Fig. 9(b), Fig. 10(a), Fig. 10(b), respectively. The phenomena of wave propagation in OA media can be explained theoretically by solving the Christoffel equation [32, 35].
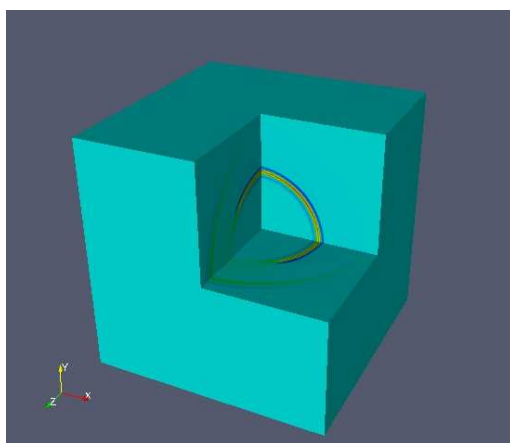

Figure 11: A snapshot of 3-D wave propagation in an orthorhombic anisotropy medium at a propagation time 0.38s. It is a 3-D data volume of displacement w.

4   Conclusions

Wave simulation of propagation in elastic media is an important topic in oil geological exploration or inverse problems. In this paper, the pseudospectral method is used for wave simulation in 3-D elastic anisotropic media. The pseudospectral method calculates spatial derivatives by the fast Fourier transform in stead of finite differences, while time
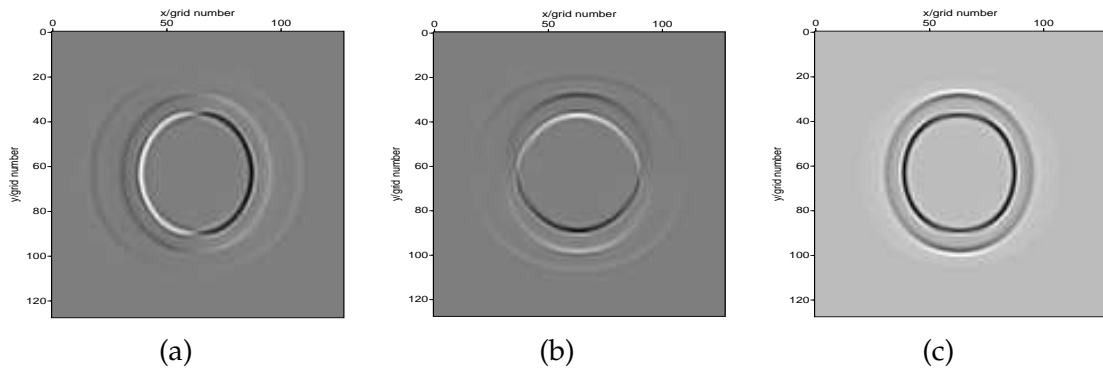
Figure 12: Wavefront of wave propagation in an orthorhombic media in the xy plane with the z directional point source. (a) x component, (b) y component, (c) z component.
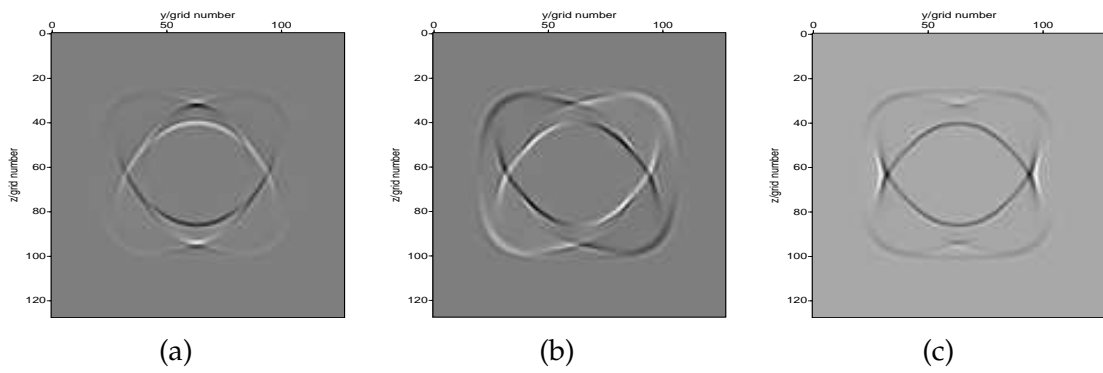

Figure 13: Wavefront of wave propagation in an orthorhombic medium in the yz plane with the z directional point source. (a) x component, (b) y component, (c) z component.
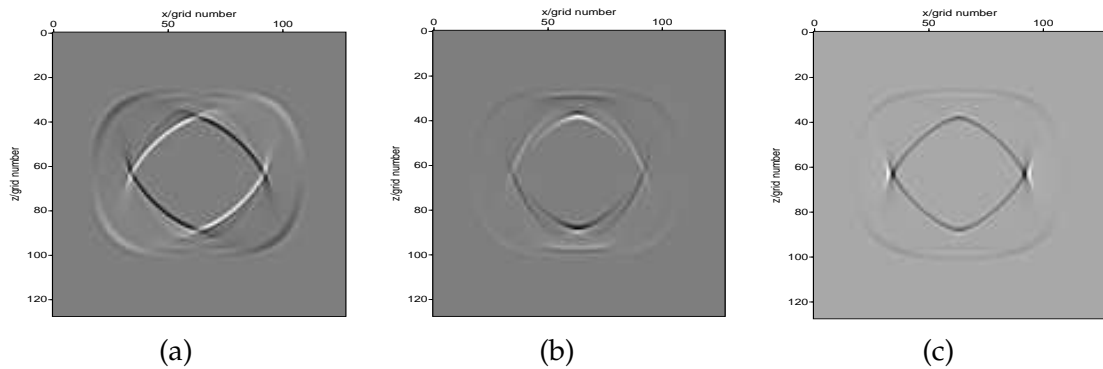

Figure 14: Wavefront of wave propagation in an orthorhombic medium in the xz plane with the z directional point source. (a) x component, (b) y component, (c) z component.

derivatives appeared in wave equations are calculated by the second-order difference scheme. The stability conditions for wave simulation in 3-D anisotropic media are investigated in detail. The stability conditions can be expressed explicitly by the corresponding

elastic constants which are easy to use in computations. Numerical computations for two typical anisotropic media, transversely isotropic (IT) media and orthorhombic anisotropy (OA) media, are completed. The phenomena of wave propagation is shown clearly.

Acknowledgments

References

[1] R. M. Alford, K. R. Kelly and D. M. Boore, Accuracy of finite-difference modeling of acoustic wave equations, Geophysics, 39 (1974), 834-842.
[2] K. Aki and P. G. Richards, Quantitative Seismology: Theory and Methods, W. H. Freeman and Company, San Francisco, 1980.
[3] B. A. Auld, Acoustic Fields and Elastic Waves in Solids, Wiley, 1973.
[4] E. Bécache, P. Joly and C. Tsogka, An analysis of new mixed finite elements for the approximation of wave propagation problems, SIAM J. Numer. Aanl., 37 (2000), 1053-1084.
[5] J. M. Carcione, D. Kosloff, A. Behle and G. Seriani, A spectral scheme for wave propagation simulation in 3-D elastic-anisotropic media, Geophysics, 57 (1992), 1593-1607.
[6] E. T. Chung and B. Engquist, Optimal discontinuous Galerkin methods for wave propagation, SIAM J. Numer. Anal., 44 (2006), 2131-2158.
[7] E. T. Chung and B. Engquist, Optimal discontinuous Galerkin methods for the acoustic wave equation in higher dimensions, SIAM J. Numer. Anal., 47 (2009), 3820-3848.
[8] V. Červený, I. Molotkov and I. Pšenčik, Ray Methods in Seismology, University Karbva, Praha, 1977.
[9] G. Cohen, P. Joly, J. E. Roberts and N. Tordjman, Higher order triangular finite elements with mass lumping for the wave equations, SIAM J. Numer. Anal., 38 (2001), 2047-2078.
[10] F. Collino and C. Tsogka, Application of the perfectly matched absorbing layer model to the linear elastodynamic problem in anisotropic heterogeneous media, Geophysics, 66 (2001), 294-307.
[11] E. Dormy and A. Tarantola, Numerical simulation of elastic wave propagation using a finite volume method, J. Geophys. Res., 100 (1995), 2123-2133.
[12] E. L. Faria and P. L. Stoffa, Finite-difference modeling in transversely isotropic media, Geophysics, 59 (1994), 282-289.
[13] B. Fornberg, On a Fourier method for the integration of hyperbolic equations, SIAM J. Numer. Anal., 12 (1975), 509-528.
[14] B. Fornberg, The pseudospectral method: comparisons with finite differences for the elastic wave equation, Geophysics, 52 (1987), 483-501.
[15] B. Fornberg, The pseudospectral method: accurate representation of interfaces in elastic wave calculations, Geophysics, 53 (1988), 625-637.

[16] D. Gajewski and I. Pšenčik, Computation of high frequency seismic wavefields in 3-D later-ally inhomogeneous anisotropic media, Geophys. J. Roy. Astr. Soc., 91 (1987), 383-411.

[17] G. H. Golub and C. F. Van Loan, Matrix Computations (3rd ed.), Johns Hopkins University Press, 1996.

[18] H. Igel, P. Mora and B. Riollet, Anisotropic wave propagation through finite-difference grids. Geophysics, 60 (1995), 1203-1216.

[19] A. Jerri, The Shannon sampling theorem – its various extensions and applications: a tutorial review, Proceedings of the IEEE, 65 (1977), 1565-1596.

[20] K. R. Kelly, R. W. Ward, S. Treitel and R. M. Alford, Synthetic seismograms: a finite-difference approach, Geophysics, 41 (1976), 2-27.

[21] D. D. Kosloff and E. Baysal, Forward modeling by a Fourier method, Geophysics, 47 (1982), 1402-1412.

[22] K. J. Marfurt, Accuracy of finite-difference and finite-element modelling of the scalar and elastic wave equations, Geophysics, 49 (1984), 535-549.

[23] J. J. H. Miller, On the location of zeros of certain classes of polynomials with applications to numerical analysis, IMA J. Appl. Math., 8 (1971), 397-406.

[24] W. A. Mulder, A comparison between high-order finite elements and finite differences for solving the wave equation, Proc. 2nd ECCOMAS Conf. on Numerical Methods in Engineer-ing, John Wiley & Sons, Paris, 1996, 344-350.

[25] S. Nilsson, N. A. Petersson, B. Sjörn and H. Kreiss, Stable difference approximations for the elastic wave equation in second order formulation, SIAM J. Numer. Anal., 45 (2007), 1902-1936.

[26] S. A. Orszag, Spectral methods for problems in complex geometries, J. Comp. Phys., 39 (1980), 70-92.

[27] A. T. Patera, A spectral element method for fluid dynamics: Laminar flow in a channel expansion, J. Comp. Phys., 54 (1984), 468-488.

[28] R. G. Payton, Elastic wave propagation in transversely isotropic media, Martinus Nijhoff Publishers, 1983.

[29] M. Reshef, D. Kosloff, M. Edwards and C. Hsiung, Three-dimensional acoustic modeling by the Fourier method, Geophysics, 53 (1988), 1175-1183.

[30] M. Reshef, D. Kosloff, M. Edwards and C. Hsiung, Three dimensional elastic modeling by the Fourier method, Geophysics, 53 (1988), 1184-1193.

[31] C. M. Sayers and D. A. Ebrom, Seismic traveltime analysis of azimuthally anisotropic media: Theory and experiment, Geophysics, 62 (1997), 1570-1582.

[32] M. Schoenberg and K. Helbig, Orthorhombic media: Modelling elastic wave behavior in a vertically fractured earth, Geophysics, 62 (1997), 1954-12974.

[33] G. Seriani and E. Priolo, Spectral element method for acoustic wave simulation in heteroge-neous media, Finite Elements in Analysis and Design, 16 (1994), 337-348.

[34] J. W. Thomas, Numerical Partial Difference Equations: Finite Difference Methods, Springer-Verlag New York Inc., 1995.

[35] I. Tsvankin, Anisotropic parameters and P-wave velocity for orthorhombic media, Geo-physics, 62 (1997), 1292-1309.

[36] C. Tsingas, A. Vafidis and E. R. Kanasewich, Elastic wave propagation in transversely isotropic media using finite differences, Geophys. Prosp., 38 (1990), 933-949.

[37] J. Virieux, P-SV wave propagation in heterogeneous media: velocity-stress finite-difference method, Geophysics, 51 (1986), 889-901.

[38] D. Yang, E. Liu, Z. Zhang and J. Teng, Finite-difference modelling in two-dimensional

anisotropic media using a flux-corrected transport technique, Geophys. J. Int., 148 (2002), 320-328.

[39] D. Yang, G. Song and M. Lu, Optimally accurate nearly analytic discrete scheme for wave-field simulation in 3D anisotropic media, Bulletin of the Seismological Society of America, 97 (2007), 1557-1569.

[40] O. C. Zienkiewicz, R. L. Taylor and J. Z. Zhu, The Finite Element Method – its Basis and Fundamentals (6th ed.), Elsevier Butterworth-Heinemann, 2005.

[41] J. F. Zhang, Elastic wave modeling in fractured media with an explicit approach, Geophysics, 70 (2005), T75-T85.

[42] W. S. Zhang and Q. D. He, Pseudo-spectral forward modeling in transversally isotropic medium, Oil Geophysical Prospecting, 33 (1998), 310-319 (in Chinese).